Springer

Journal of
Mechanical
Science and
Technology

Journal of Mechanical Science and Technology 23 (2009) 624~630

www.springerlink.com/content/1738-494x
DOI 10.1007/s12206-008-1211-1

Measurement of the heat transfer coefficient in the dimpled channel: effects of dimple arrangement and channel height †

Somin Shin[1], Ki Seon Lee[1], Seoung Duck Park[1] and Jae Su Kwak[2,*]

[1]*Graduate student, School of Aerospace and Mechanical Engineering, Korea Aerospace University, Goyang City, Kyung-Gi Do,, Korea*

[2]*Assistant Professor, School of Aerospace and Mechanical Engineering, Korea Aerospace University, Goyang City, Kyung-Gi Do,, Korea*

(Manuscript Received January 25, 2008; Revised July 3, 2008; Accepted December 14, 2008)

Abstract

Heat transfer coefficients were measured in a channel with one side dimpled surface. The sphere type dimples were fabricated, and the diameter (D) and the depth of dimple was 16 mm and 4 mm, respectively. Two channel heights of about 0.6D and 1.2D, two dimple configurations were tested. The Reynolds number based on the channel hydraulic diameter was varied from 30000 to 50000. The improved hue detection based transient liquid crystal technique was used in the heat transfer measurement. Heat transfer measurement results showed that high heat transfer was induced downstream of the dimples due to flow reattachment. Due to the flow recirculation on the upstream side in the dimple, the heat transfer coefficient was very low. As the Reynolds increased, the overall heat transfer coefficients also increased. With the same dimple arrangement, the heat transfer coefficients and the thermal performance factors were higher for the lower channel height. As the distance between the dimples became smaller, the overall heat transfer coefficient and the thermal performance factors increased.

Keywords: Turbine heat transfer; Turbine blade cooling; Dimple; Transient liquid crystal technique

1. Introduction

It is known that the efficiency and power output of gas turbine engines increases as the turbine inlet temperature increases. Also, the operating temperature of modern gas turbines goes beyond the permissible temperature of turbine blade materials. Given these conditions a sophisticated cooling system is required in order to maintain durability and required lifetime of the turbine blades.

A blade cooling system could be selected by considering degree of heat transfer augmentation, pressure drop through the cooling channel, and manufacturing simplicity. It is known that the dimpled surface increases heat transfer with a lower pressure drop compared to the rib turbulated cooling technique which is widely used in gas turbine blades. Furthermore a surface with dimples is easy to fabricate. Thus, a heat transfer augmenting technique using dimples has been tried as a blade cooling system in gas turbines.

Dimples fabricated on the surface of blades increase heat transfer because it induces flow separation, reattachment, and vortices. Khalatov et al. [1] visualized the flow near dimples by dye injection. Mahmood et al. [2] used infrared thermography and presented flow visualization, time-averaged total pressure, streamwise velocity, and spatially resolved local Nusselt numbers near the dimple. Mahmood and Ligrani [3] presented the influences of dimples on flow structure and heat transfer on different channel aspect ratios, different inlet air-to-local wall temperature ratios, and Reynolds numbers. Burgess and Ligrani [4] investigated friction

† This paper was recommended for publication in revised form by Associate Editor Yong Tae Kang

*Corresponding author. Tel.: +82 2 300 0103, Fax.: +82 2 3158 3189
E-mail address: jskwak@kau.ac.kr

factors and Nusselt number based on dimple depth. Moon and Lau [5] examined the effect of dimple geometry on the convective heat transfer and pressure drop in a square channel with an array of concave or cylindrical dimples. Moon et al. [6] measured heat transfer coefficients in the four different channel heights, and friction factors using static pressure taps. Ligrani et al. [7] investigated the effect of dimple depth and inlet turbulence intensity on the Nusselt number and friction factors. Chyu et al. [8] studied local heat transfer distribution on the surfaces with hemispheric and tear-drop shapes of concavities using a transient liquid crystal imaging system. Ligrani et al. [9] experimented with a channel with a dimpled surface on one wall, both with and without protrusions on the opposite wall, while Borisov et al. [10] studied the channel with dimple concavities on both sides.

Most literature has presented the averaged Nusselt number or local Nusselt number distribution with low resolution. In this paper, in order to investigate the detailed heat transfer augmentation using dimples, the improved transient liquid crystal technique was used to measure the detailed local heat transfer coefficient distribution in and near the dimples fabricated on a flat surface. The quality of the measured heat transfer coefficient by the transient liquid crystal technique was improved by the time-hue curve fitting method and the analytical solution for the varying mainstream temperature condition. The presented measurement results will clearly show high and low heat transfer regions by the dimple-induced flow phenomena.

2. Experiment set up

The test facility consisted of a venturi flow meter with a differential pressure transmitter (Rosemount, 250in H_2O), a blower (p_{max}=4800mmH_2O, Q_{max}= 9.8m^3/min), an electrical heater (12kW), and two pneumatic valves. Fig. 1 shows the schematic of the test facility. The test section was made of 10 mm transparent polycarbonate plate. The flow rate was measured by a Venturi flow meter and calculated by Eq. (1). (ISO, [11])

$$Q = \frac{C_d}{\sqrt{1-\beta^4}} \varepsilon \frac{1}{4} \pi d^4 \sqrt{\frac{2\Delta p}{\rho}} \quad (1)$$

Heated air is bypassed until the air temperature reaches a predetermined value. After the air temperature reaches the predetermined value, the air is diverted to the test section by pneumatic valves. Thermocouples or pressure taps were installed at the beginning and end of the arrayed dimples to measure mainstream temperature and pressure drop through the dimpled region. Black paint and liquid crystals with a bandwidth of 1℃ (35C1W, Hallcrest) were sprayed on the heat transfer measurement planes, and a digital CCD camera and incandescent lamps were installed above the test section. During the heat transfer measurement, the color change of liquid crystals was stored in a computer through IEEE1394 cable at a rate of 30 frames per second (DV format AVI file). Using every pixel of each frame of the AVI file, RGB(red, green, and blue) values were calculated and converted to 8 bit HSI(hue, saturation, and intensity). The hue history on each pixel was curve-fitted in order to calculate the transient time between the test start and the time at which the hue value becomes the preset value. All image processes were conducted by the Matlab-based image processing program devel-

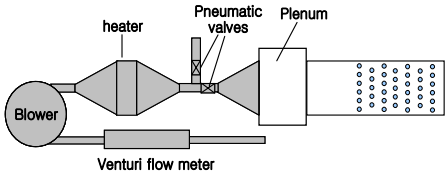

Fig. 1. Schematic of test facility (not to scale).

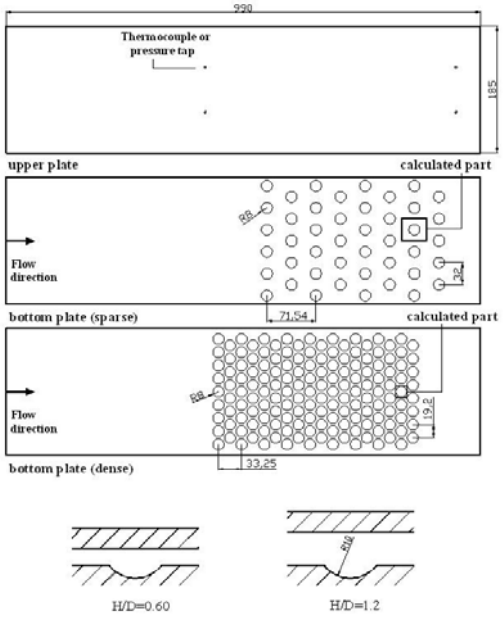

Fig. 2. Configuration of test section.

oped by the authors. By using the time-hue curve fitting method, the unstable hue behavior under low intensity conditions and noise effect on the hue by the image capturing system can be reduced and more accurate transient time can be evaluated. Detailed image processing procedures were described by Shin et al. [12].

During the transient tests, the change of the mainstream temperature was measured by 4 T-type thermocouples and recorded by a data acquisition device (Agilent, 34970A). Fig. 2 presents the configuration of the test section. The diameter (D) and depth of the dimples were 16 mm and 4 mm, respectively. The channel height (H) to the diameter of the dimple was 0.6 and 1.2, and two dimple arrangements shown in Fig. 2 were tested.

3. Measurement theory

In the transient liquid crystal technique, the test surface is assumed as a semi-infinite solid wall with a convective boundary condition. If the sudden change in mainstream temperature or velocity is applied to the test section, the surface temperature changes with time and the heat transfer coefficient can be calculated by utilizing the time between the initial temperature and the preset surface temperature. The basic equation, initial, and boundary conditions are as follows:

$$k_w \frac{\partial^2 T}{\partial x^2} = \rho_w c_p \frac{\partial T}{\partial t} \tag{2}$$

$$at \;\; t = 0, \; T = T_i \tag{3}$$

$$at \;\; x = 0, \; -k_w \frac{\partial T}{\partial x} = h(T_w - T_m) \tag{4}$$

$$as \;\; x \to \infty, T = T_i \tag{5}$$

If the mainstream temperature varies with time, which commonly occurs in internal heat transfer tests, temperature variations of the mainstream can be expressed as shown in Eq. (6) (Kwak, [13]).

$$\theta_m = T_m - T_i = \sum_{n=1}^{N} a_n \frac{t^{n-1}}{\Gamma(n)} \tag{6}$$

Where, N=n+1

Temperature variations on the surface (x=0) can be expressed as Eq. (7).

$$\theta_w = T_w - T_i = \sum_{n=1}^{N} a_n \left[\sum_{m=1}^{n} \frac{1}{\beta_p^{\,2(m-1)}} \frac{t^{n-m}}{(n-m)!} - \frac{1}{\beta_p^{\,2(n-1)}} e^{t\beta_p^2} erfc\left(\beta_p \sqrt{t}\right) - \sum_{i=1}^{n-1} \frac{1}{\beta_p^{\,2i-1}} \frac{2^{n-i} \; t^{n-i-\frac{1}{2}}}{\left(1 \cdot 3 \cdot 5 \cdot 7 \cdots\cdots [2(n-i)-1]\right)\sqrt{\pi}} \right] \tag{7}$$

where $\beta_p = \dfrac{h\sqrt{\alpha}}{k}$

Once the time (t) from the initial temperature (T_i) to the pre-defined temperature (T_w) is determined, the heat transfer coefficient can be calculated by Eq. (7).

The mainstream temperature is curve-fitted by using an averaged temperature measured by T-type thermocouples installed at the beginning and the end of the dimple fabricated region. The mainstream temperature for the heat transfer calculation at each pixel was calculated based on the distance between the thermocouples and the location of each pixel.

The surface temperature was obtained from pre-operated hue-temperature calibrations. For the hue-temperature calibration, a copper plate was attached on the hot side of thermoelectric element with high conductive glue. A T-type thermocouple was instrumented on the copper plate and a 1℃ bandwidth of liquid crystals (35C1W, Hallcrest) was sprayed on the copper plate after black paint was applied on. By changing the temperature of the copper plate by 0.2℃ steps, the color of the liquid crystal coated surface was recorded and a hue value was calculated. Fig. 3 shows the relation between the calculated hue and the temperature obtained by the thermocouple couple.

Augmentation of heat transfer by dimpled surface accompanies a pressure drop. Thus, the heat transfer

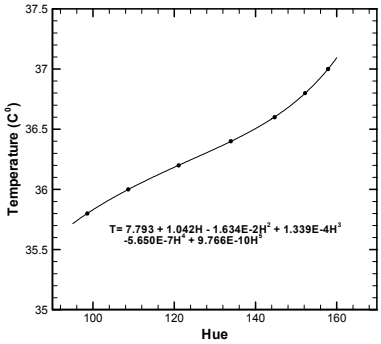

Fig. 3. Relation between temperature and hue.

augmentation should be compared with the pressure drop in order to evaluate the thermal performance of heat transfer enhancing methods. In this study, the thermal performance factor defined by Eq. (8) was used.

$$TP = \frac{\overline{Nu}_{D_h} / Nu_{D_h,0}}{\left(f / f_0\right)^{1/3}} \tag{8}$$

In Eq. (8), f_0 is the friction factor for fully developed turbulent flow in a smooth tube, f is the Darcy friction factor calculated from pressure measurement, $Nu_{Dh,0}$ is the Nusselt number for fully developed turbulent flow in smooth tubes with the same hydraulic diameter, and Nu_{Dh} is the measured Nusselt number. The Darcy friction factor, f is defined by Eq. (9).

$$f = \frac{-(\Delta p / \Delta x) D_h}{\rho_m \, \overline{u}^2 / 2} \tag{9}$$

In Eq. (9), the pressure drop, Δp, was measured by four pressure taps shown in Fig. 2, and f_0 was calculated by Eq. (10) (Frank and David [14]).

$$f_0 = \left[0.79 \ln(\mathrm{Re}_{D_h}) - 1.64\right]^{-2} \tag{10}$$

for $3000 < \mathrm{Re}_{D_h} < 5 \times 10^6$

The averaged Nusselt number is defined in Eq. (11) and the Nusselt number for smooth tubes, $Nu_{Dh,0}$ can be calculated by Eq. (12) (Frank and David [14]), respectively.

$$\overline{Nu}_{Dh} = \frac{\overline{h} D_h}{k_m} \tag{11}$$

$$Nu_{D_h,0} = \frac{(f_0/8)(\mathrm{Re}_{D_h} - 1000)\,\mathrm{Pr}}{[1 + 12.7(f_0/8)^{1/2}(\mathrm{Pr}^{2/3} - 1)]} \tag{12}$$

for $0.5 < \mathrm{Pr} < 2000$ and $3000 < \mathrm{Re}_{D_h} < 5 \times 10^6$

Measurement uncertainty in the heat transfer coefficient was estimated numerically (Dunn, [15]) since Eq. (7) can not be expressed in explicit form regarding the heat transfer coefficient. The estimated uncertainty for the heat transfer coefficient and the Nusselt number was 8.13% and 9.56%, respectively.

4. Results and discussions

Various flow phenomena are induced by the dimples as shown in Fig. 4(Griffith et al. [16]). The boundary layer of the mainstream was separated by the dimples and recirculation zone is created in the upstream side of the dimples. The separated mainstream flow reattaches in the downstream side of the dimple surface and the reattached flow forms a twin vortex. As the flow comes out of the dimple, it reattaches again at the downstream of the dimple (Khalatov et al. [1], Mahmood et al. [2], Ligrani et al. [9]). These complex flow phenomena induce high and low heat transfer in and near the dimples.

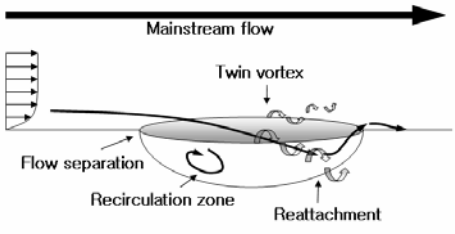

Fig. 4. Dimple induced flow phenomena.

Fig. 5 shows the distribution of the Nusselt numbers for sparsely distributed dimples (S=2D). Reynolds numbers shown in Fig. 5 are based on the averaged mainstream flow velocity and channel hydraulic diameter. Results show that the overall Nusselt number increases as the Reynolds number increases. Also, the Nusselt numbers for the lower channel height cases are higher than those for the higher channel height cases. For the same Reynolds number, the mainstream velocity is higher for the lower channel height cases, which results in higher Nusselt numbers for the lower channel height cases. Also, the higher Nusselt number for lower channel height cases was partly caused by the enhanced flow disturbance. As the ratio of channel height to dimple diameter decreases, the flow is increasingly disturbed by the dimples, which causes a higher Nusselt number. Fig. 5 also clearly shows the high and low heat transfer regions in and downstream of the dimple. Due to flow recirculation, the heat transfer coefficients upstream of the dimple are low. The heat transfer coefficients downstream of the dimple are higher because of the flow reattachment. High heat transfer coefficients along the dimple edges can be seen for about 2/3 of the dimple upstream edge. It is claimed that the high heat transfer region along the rim is caused by the twin vortices and flow reattachment. As the flow comes out from the dimple, the flow reattaches again

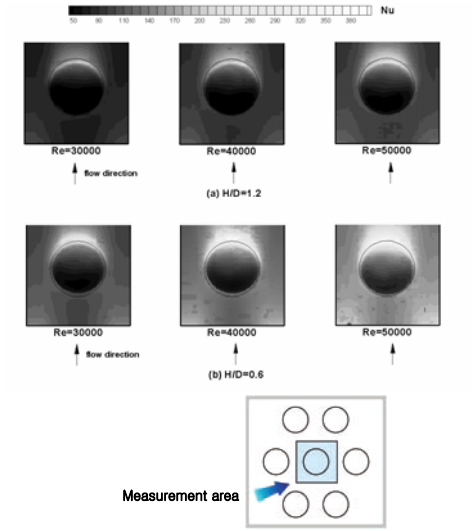

Fig. 5. Nusselt number distribution on dimpled surface (S=2D).

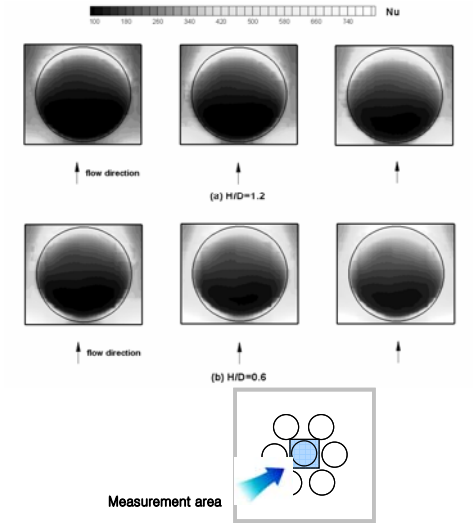

Fig. 6. Nusselt number distribution on dimpled surface (S=1.1D).

on the surface and causes a high heat transfer region downstream of the dimple.

Fig. 6 presents the distribution of the Nusselt number for densely distributed dimples (S=1.1D). The overall distribution of the Nusselt number is similar to the sparsely distributed dimple case (Fig. 5). For the same Reynolds number and channel height, the Nusselt number for the densely distributed case is higher than that of the sparsely distributed dimple case. As the distance between dimples is reduced, more flow

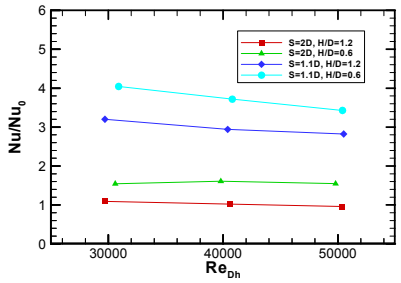

Fig. 7. Nusselt number ratio.

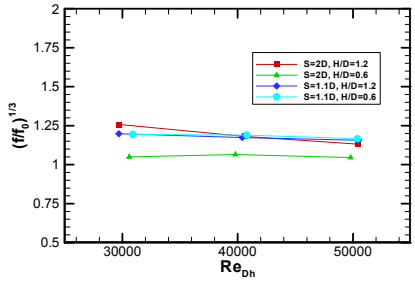

Fig. 8. Friction factor ratio.

disturbance is caused by the dimples, which results in an increase in heat transfer.

Fig. 7 shows the averaged Nusselt number on the dimpled surface compared to a smooth tube with the same hydraulic diameter. Generally, the Nusselt number ratio decreases as the Reynolds number increases. For the same Reynolds number, the lower channel height case shows a higher Nusselt number ratio and the densely distributed dimples induced a higher Nusselt number ratio. Thus, the highest Nusselt number ratio was obtained from the densely distributed dimples with a low channel height.

Fig. 8 presents the friction factor ratio compared to a smooth tube with the same hydraulic diameter. Generally, the friction factor ratio decreases as the Reynolds number increases. Actual pressure drop is higher for the higher Reynolds number case, but the difference in the friction factor ratio is not significant.

The thermal performance factor generally decreases as the Reynolds number increases (Fig. 9). However, the amount of change is not significant. The thermal performance factor depends more on the arrangement of dimples and the channel height. Thus, the thermal performance of the dimpled surface can be optimized by changing the channel height to dimple diameter ratio or the arrangement of the dimples. In this study, one dimple depth was tested, but it is expected that the depth of dimple is one of the impor-

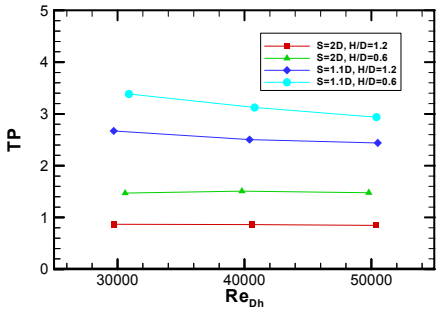

Fig. 9. Thermal performance factor.

tant factors of heat transfer augmentation with dimpled surfaces. The optimization of the dimple configuration and arrangement will be the next step of this study.

5. Conclusions

The distribution of the heat transfer coefficient on the dimpled surface was measured by an improved transient liquid crystal technique. Two configurations of dimples were tested and for each configuration, channel height to dimple diameter ratio was set at 0.6 and 1.2, and depth of the dimple was 1/4 of the dimple diameter.

Results showed that the heat transfer coefficient upstream side of the dimple was low because of flow recirculation. Similarly, a high heat transfer region was found downstream of the dimple due to flow reattachment. The heat transfer coefficient increased as the Reynolds number increased, and the lower channel height cases showed higher a heat transfer coefficient. Also, the heat transfer coefficient was higher for the densely distributed dimple case. The thermal performance factor was generally larger than 1 and the highest thermal performance factor was over 3 for the lower channel height and densely distributed dimple case.

It was clearly shown that the configuration of the dimples and channel height could be optimized in order to increase the thermal performance factor. The other possible performance factors such as depth or shape of dimple will be considered in following studies.

Acknowledgment

This study has been supported by the KARI under KHP Dual-Use Component Development Program funded by the MOCIE and the Korea Research Foundation Grant funded by the Korean Government (MOEHRD, Basic Research Promotion Fund) (KRF-2007-331-D00068).

References

[1] A. Khalatov, A. Byerley, D. Ochoa and M. Seong-Ki, Flow characteristics within and downstream of spherical and cylindrical dimple on a flat plate at low Reynolds numbers, ASME paper GT2004-53656 (2004).

[2] G. I. Mahmood, M. L. Hill, D. L. Nelson and P. M. Ligrani, Local heat transfer and flow structure on and above a dimpled surface in a channel, ASME paper 2000-GT-230 (2000).

[3] G. I. Mahmood and P. M. Ligrani, Heat transfer in a dimpled channel: combined influences of aspect ratio, temperature ratio, Reynolds number, and flow structure, *International J. of Heat and Mass Transfer*, pp. 2011-2020 (2002).

[4] N. K. Burgess and P. M. Ligrani, Effects of dimple depth on Nusselt numbers and friction factors for internal cooling in a channel, ASME paper GT2004-54232 (2004).

[5] S. W. Moon and S. C. Lau, Turbulent heat transfer measurements on a wall with concave and cylindrical dimples in a square channel, ASME paper GT-2002-30208 (2002).

[6] H. K. Moon, T. O'Connell and B. Glezer, Channel height effect on heat transfer and friction in a dimpled passage, *J. of Engineering for Gas Turbines and Power*, 122 (2000) 307-313.

[7] P. M. Ligrani, N. K. Burgess and S. Y. Won, Nusselt numbers and flow structure on and above a shallow dimpled surface within a channel including effects of inlet turbulence intensity level, ASME paper GT-2004-54231 (2004).

[8] M. K. Chyu, Y. Yu, H. Ding, J. P. Downs and F. O. Soechting, Concavity enhanced heat transfer in an internal cooling passage, ASME paper 97-GT-437 (1997).

[9] P. M. Ligrani, G. I. Mahmood, J. I. Harrison, C. M. Clayton and D. L. Nelson, Flow structure and local Nusselt number variations in a channel with dimples and protrusions on opposite walls, *International J. of Heat and Mass Transfer*, 4413-4425 (2001).

[10] I. Borisov, A. Khalatov and S. Kobzar, Comparison of thermo-hydraulic characteristics for two

types of dimpled surfaces, ASME paper GT2004-54204 (2004).

[11] ISO, Measurement of fluid flow by means of pressure differential devices inserted in circular cross-section conduits running full-Part 4: Venturi tubes, ISO 5167-4 (2004).

[12] S. Shin, C. S. Jeon, J. S. Kwak and Y. W. Jung, Improvement of accuracy in evaluating hue change time in the hue detection based transient liquid crystals technique, *Transaction of KSME B*, 31 (11) (2007) 918-915.

[13] J. S. Kwak, Comparison of analytical and superposition solutions of the transient liquid crystal technique, *Journal of Thermophysics and Heat Transfer*, 22 (2) (2008) 290-295.

[14] P. I. Frank and P. D. David, *Fundamentals of Heat and Mass Transfer*, Wiley, pp. 470-492 (2001)

[15] Dunn, P. F., 2005, *Measurement and data analysis for engineering and science*, McGraw-Hill, Inc.

[16] T. S. Griffith, L. Al-Hadhrami and J. C. Han, Heat transfer in rotating rectangular cooling channels (AR=4) with dimples, ASME paper GT-2002-30220 (2002).

Jae Su Kwak received his B.S. and M.S. degrees in Mechanical Engineering from Korea University in 1996 and 1998, respectively. He then received his Ph.D. from Texas A&M University in 2002. Dr. Kwak is currently an Assistant Professor at the School of Aerospace and Mechanical Engineering at Korea Aerospace University in Goyang-City, Korea. His main research interests include gas turbine heat transfer, compact heat exchanger, and enhancement of heat transfer.